Leptoquark Production and Identification in High Energy $\mu^+\mu^-$, e^+e^- and $e\gamma$ Collisions*

Michael A. Doncheski[1] and Stephen Godfrey[2]
[1]*Department of Physics, Pennsylvania State University, Mont Alto, PA 17237 USA*
[2]*Ottawa-Carleton Institute for Physics*
Department of Physics, Carleton University, Ottawa CANADA, K1S 5B6

ABSTRACT

We study single leptoquark production in e^+e^-, $e\gamma$, and $\mu^+\mu^-$ collisions due to the quark content of the photon. Leptoquarks can be produced in substantial numbers for masses very close to the centre of mass energy of the collider which results in equivalently high discovery limits. Using polarization asymmetries in an $e\gamma$ collider the ten different types of leptoquarks listed by Buchmüller, Rückl and Wyler can be distinquished from one another for leptoquark masses essentially up to the kinematic limit. Thus, if a leptoquark were discovered an $e\gamma$ collider could play a crucial role in determining its origins.

I. INTRODUCTION

There is considerable interest in the study of leptoquarks (LQs) — colour (anti-)triplet, spin 0 or 1 particles which carry both baryon and lepton quantum numbers. Such objects appear in a large number of extensions of the standard model such as grand unified theories, technicolour, and composite models. Quite generally, the signature for leptoquarks is very striking: a high p_T lepton balanced by a jet (or missing p_T balanced by a jet, for the νq decay mode, if applicable). Searches for leptoquarks have been performed by the H1 [1] and ZEUS [2] collaborations at the HERA ep collider, by the D0 [3] and CDF [4] collaborations at the Tevatron $p\bar{p}$ collider, and by the ALEPH [5], DELPHI [6], L3 [7], and OPAL[8] collaborations at the LEP e^+e^- collider. Discovery limits have also been obtained for the LHC[9]. In this report we consider single leptoquark production in $\mu^+\mu^-$, e^+e^-, and $e\gamma$ collisions which utilizes the quark content of either a backscattered laser photon for the $e\gamma$ case or a Weizacker-Williams photon radiating off of one of the initial leptons for the $\mu^+\mu^-$ or e^+e^- cases [10, 11, 12, 13, 14, 15, 16]. This process offers the advantage of a much higher kinematic limit than the LQ pair production process, is independent of the chirality of the LQ, and gives similar results for both scalar and vector leptoquarks. In the first part of this report we use single leptoquark production to estimate the discovery limits at future high energy $\mu^+\mu^-$, e^+e^-, and $e\gamma$ colliders.

Although the discovery of a leptoquark would be dramatic evidence for physics beyond the standard model it would lead to the question of which model the leptoquark originated from. Given the large number of leptoquark types it would be imperative to measure its properties to answer this question. There are 10 distinct leptoquark types which have been classified by Buchmüller, Rückl and Wyler (BRW) [17]: S_1, $\tilde{S}_1$ (scalar, iso-singlet); R_2, $\tilde{R}_2$ (scalar, iso-doublet); S_3 (scalar, iso-triplet); U_1, $\tilde{U}_1$ (vector, iso-singlet); V_2, $\tilde{V}_2$ (vector, iso-doublet); U_3 (vector, iso-triplet). The production and corresponding decay signatures are quite similar, though not identical, and have been studied separately by many authors. The question arises as to how to differentiate between the different types. In the second part of this report we show how a polarized $e\gamma$ collider can be used to differentiate the LQs. (ie. a polarized e beam, like SLC, in conjunction with a polarized-laser backscattered photon beam.) This process takes advantage of the hadronic component of the photon which is important and cannot be neglected [18].

II. LEPTOQUARK PRODUCTION

The process we are considering is shown if Fig. 1. The parton level cross section for scalar leptoquark production is trivial, given by:

$$\sigma(\hat{s}) = \frac{\pi^2 \kappa \alpha_e m}{M_s} \delta(M_s - \sqrt{\hat{s}}) \tag{1}$$

where we have followed the convention adopted in the literature[13] where the leptoquark couplings are replaced by a generic Yukawa coupling g which is scaled to electromagnetic strength $g^2/4\pi = \kappa\alpha_{em}$. The cross section for vector leptoquark production is a factor of two larger. We only consider generation diagonal leptoquark couplings so that only leptoquarks which couple to electrons can be produced in $e\gamma$ (or e^+e^-) collisions while for the $\mu^+\mu^-$ collider only leptoquarks which couple to muons can be produced. Convoluting the parton level cross section with the quark distribution in the photon one obtains the expression

$$\begin{aligned} \sigma(s) &= \int f_{q/\gamma}(z, M_s^2)\hat{\sigma}(\hat{s})dz \\ &= f_{q/\gamma}(M_s^2/s, M_s^2)\frac{2\pi^2\kappa\alpha_{em}}{s}. \end{aligned} \tag{2}$$

The cross section depends on the LQ charge since the photon has a larger u quark content than d quark content. We note that the interaction Lagrangian used in Ref. [14] associates a factor $1/\sqrt{2}$ with the leptoquark-lepton-quark coupling. Thus, one should compare our results with κ to those in Ref. [14] with 2κ. We give results with κ chosen to be 1.

For $e\gamma$, e^+e^-, and $\mu^+\mu^-$ colliders the cross section is obtained by convoluting the expression for the resolved photon contribution to $e\gamma$ production of leptoquarks, Eqn. (2), with, as appropriate, the backscattered laser photon distribution [19] or

* This research was supported in part by the Natural Sciences and Engineering Research Council of Canada.

the Weizsäcker-Williams effective photon distribution: [1]

$$\sigma(\ell^+\ell^- \to XS) = \frac{2\pi^2\alpha_{em}\kappa}{s}\int_{M_s^2/s}^1 \frac{dx}{x} f_{\gamma/\ell}(x,\sqrt{s}/2) \times f_{q/\gamma}(M_s^2/(xs), M_s^2). \quad (3)$$

Before proceeding to our results we consider possible backgrounds [20]. The leptoquark signal consists of a jet and electron with balanced transverse momentum and possibly activity from the hadronic remnant of the photon. The only serious background is a hard scattering of a quark inside the photon by the incident lepton via t-channel photon exchange; $eq \to eq$. By comparing the invariant mass distribution for this background to the LQ cross sections we found that it is typically smaller than the LQ signal by two orders of magnitude. Related to this process is the direct production of a quark pair via two photon fusion

$$e + \gamma \to e + q + \bar{q}. \quad (4)$$

However, this process is dominated by the collinear divergence which is actually well described by the resolved photon process $eq \to eq$ given above. Once this contribution is subtracted away the remainder of the cross section is too small to be a concern [20]. Another possible background consists of τ's pair produced via various mechanisms with one τ decaying leptonically and the other decaying hadronically. Because of the neutrinos in the final state it is expected that the electron and jet's p_T do not in general balance which would distinguish these backgrounds from the signal. However, this background should be checked in a realistic detector Monte Carlo to be sure. The remaining backgrounds originate from heavy quark pair production with one quark decaying semileptonically and only the lepton being observed with the remaining heavy quark not being identified as such. All such backgrounds are significantly smaller than our signal in the kinematic region we are concerned with.

III. LEPTOQUARK DISCOVERY LIMITS

In Fig. 2 we show the cross sections for a $\sqrt{s} = 1$ TeV e^+e^- operating in both the backscattered laser $e\gamma$ mode and in the e^+e^- mode. The cross section for leptoquarks coupling to the u quark is larger than those coupling to the d quark. This is due to the larger u quark content of the photon compared to the d quark content which can be traced to the larger Q_q^2 of the u-quark. There exist several different quark distribution functions in the literature [21, 22, 23, 24, 25]. For the four different leptoquark charges we show curves for three different distributions functions: Drees and Grassie (DG)[23], Glück, Reya and Vogt (GRV)[24], and Abramowicz, Charchula and Levy (LAC) set 1[25]. The different distributions give almost identical results for the $Q_{LQ} = -1/3,\ -5/3$ leptoquarks and for the $Q_{LQ} = -2/3,\ -4/3$ leptoquarks give LQ cross sections that vary by most a factor of two, depending on the kinematic region. In the remainder of our results we will use the GRV distribution functions [24] which we take to be representative of the quark distributions in the photon.

Comparing the cross sections for the two collider modes we see that the kinematic limit for the $e\gamma$ mode is slightly lower

[1] The effective photon distribution from muons is obtained by replacing m_e with m_μ.

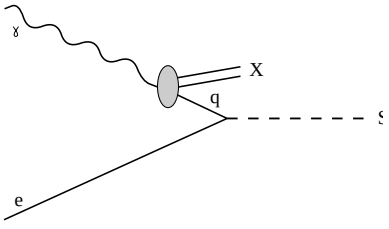

Figure 1: The resolved photon contribution for leptoquark production in $e\gamma$ collisions.

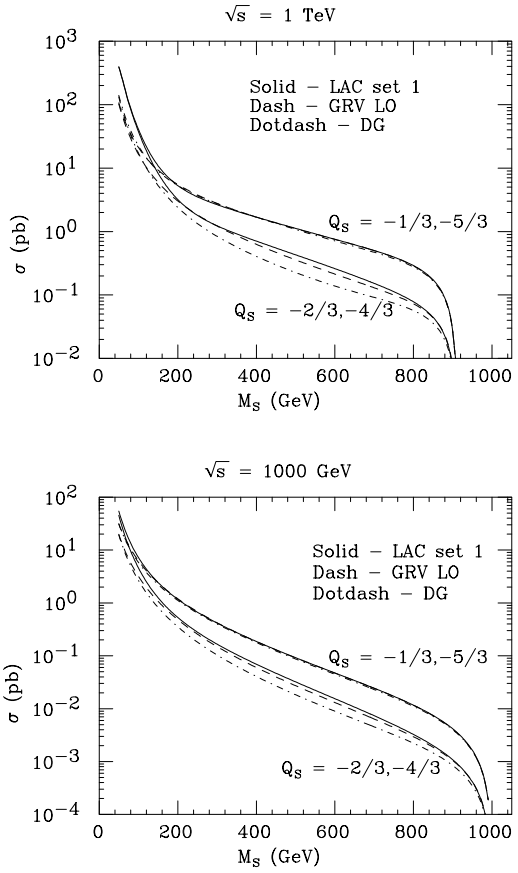

Figure 2: The cross sections for leptoquark production due to resolved photon contributions in $e\gamma$ collisions, with κ chosen to be 1. In the top figure the photon beam is due to laser backscattering in a $\sqrt{s} = 1000$ GeV e^+e^- collider. In the bottom figure the the photon distribution is given by the Weizsäcker-Williams effective photon distribution in a $\sqrt{s} = 1000$ GeV e^+e^- collider. In both cases the solid, dashed, dot-dashed line is for resolved photon distribution functions of Abramowicz, Charchula and Levy [25], Glück, Reya and Vogt [24], Drees and Grassie [23], respectively.

than the e^+e^- mode. This is because the backscattered laser mode has an inherent energy limit beyond which the laser photons pair produce electrons. On the other hand the backscattered laser cross sections is larger than the e^+e^- mode. This simply reflects that the backscattered laser photon spectrum is harder than the Weizacker-Williams photon spectrum. To determine the leptoquark discovery limits for a given collider we multiply the cross section by the integrated luminosity and use the criteria that a certain number of signature events would constitute a leptoquark discovery. When we do this we find that the discovery limits for the $e\gamma$ and e^+e^- modes are not very different. Although the $e\gamma$ mode has a harder photon spectrum, the e^+e^- mode has a higher kinematic limit.

In Fig. 3 we plot the number of events for various collider energies for e^+e^-, $e\gamma$, and $\mu^+\mu^-$ colliders. For the $\mu^+\mu^-$ collider we used the c and s quark distributions in the photon rather than the u and d quark distributions since we only consider generation diagonal leptoquark couplings. For $\sqrt{s} = 500$ GeV a e^+e^- collider will have about a 25% higher reach than a $\mu^+\mu^-$ collider due to the larger u and d distributions arising from the smaller quark masses. For the highest energy lepton colliders considered the differences become relatively small. For the high luminosities being envisaged, the limiting factor in producing enough leptoquarks to meet our discovery criteria is the kinematic limit. Because, for a given e^+e^- centre of mass energy, an e^+e^- collider will have a higher energy than an $e\gamma$ collider using a backscattered laser, the e^+e^- collider will have a higher discovery limit. Finally, note that the discovery limit for vector leptoquarks is slightly higher than the discovery limit for scalar leptoquarks. This simply reflects the fact that the cross section for vector leptoquarks is a factor of two larger than the cross section for scalar leptoquarks. We summarize the discovery limits for the various colliders in Table 1.

IV. LEPTOQUARK IDENTIFICATION

If a leptoquark were actually discovered the next step would be to determine its properties so that we could determine which model it originated from. We will assume that a peak in the $e + jet$ invariant mass is observed in some collider (*i.e.*, the existance of a LQ has been established), and so we need simply to identify the particular type of LQ. We assume that the leptoquark charge has not been determined and assume no intergenerational couplings. Furthermore, we will assume that only one of the ten possible types of LQs is present. Table 2 of BRW [17] gives information on the couplings to various quark and lepton combinations; the missing (and necessary) bit of information in BRW is that the quark and lepton have the same helicity (RR or LL) for scalar LQ production while they have opposite helicity (RL or LR) for vector LQ production. It is then possible to construct the cross sections for the various helicity combinations and consequently the double spin asymmetry [11], for the different types of LQs.

Thus, a first step in identifying leptoquarks would be to determine the coupling chirality, ie. whether it couples to e_L, e_R, or e_U. This could be accomplished by using electron polarization either directly or by using a left-right asymmetry measurement:

$$A^{+-} = \frac{\sigma^+ - \sigma^-}{\sigma^+ + \sigma^-} = \frac{C_L^2 - C_R^2}{C_L^2 + C_R^2}$$

This divides the 10 BRW leptoquark classifications into three groups:

e_L^-**:** $\tilde{R}_2, S_3, U_3, \tilde{V}_2$

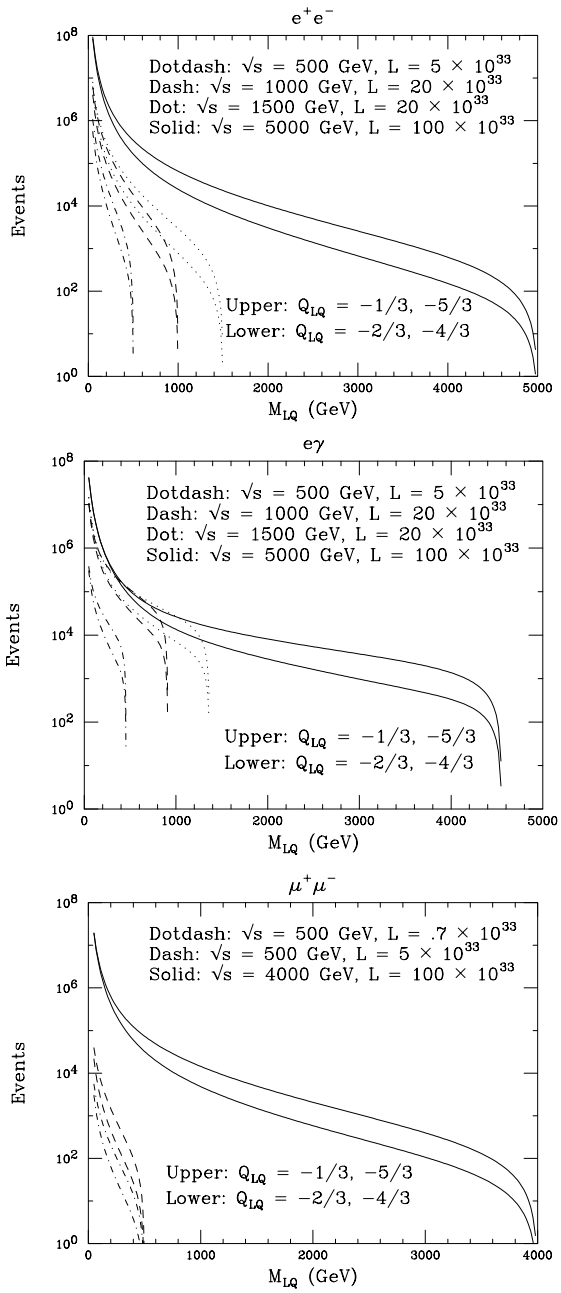

Figure 3: Event rates for single leptoquark production in e^+e^-, $e\gamma$, and $\mu^+\mu^-$ collisions. The centre of mass energies and integrated luminosities are given by the line labelling in the figures. The results were obtained using the GRV distribution functions [24].

Table I: Leptoquark discovery limits for e^+e^-, $e\gamma$, and $\mu^+\mu^-$ colliders. The discovery limits are based on the production of 100 LQ's for the centre of mass energies and integrated luminosities given in columns one and two. The results were obtained using the GRV distribution functions [24].

e^+e^- Colliders					
$\sqrt{s}$ (TeV)	L (fb^{-1})	Scalar		Vector	
		-1/3, -5/3	-4/3, -2/3	-1/3, -5/3	-4/3, -2/3
0.5	50	490	470	490	480
1.0	200	980	940	980	970
1.5	200	1440	1340	1470	1410
5.0	1000	4700	4200	4800	4500

$e\gamma$ Colliders					
$\sqrt{s}$ (TeV)	L (fb^{-1})	Scalar		Vector	
		-1/3, -5/3	-4/3, -2/3	-1/3, -5/3	-4/3, -2/3
0.5	50	450	450	450	440
1.0	200	900	900	910	910
1.5	200	1360	1360	1360	1360
5.0	1000	4500	4400	4500	4500

$\mu^+\mu^-$ Colliders					
$\sqrt{s}$ (TeV)	L (fb^{-1})	Scalar		Vector	
		-1/3, -5/3	-4/3, -2/3	-1/3, -5/3	-4/3, -2/3
0.5	0.7	250	170	310	220
0.5	50	400	310	440	360
4.0	1000	3600	3000	3700	3400

e_R^-: $\tilde{S}_1, \tilde{U}_1$

e_U^-: U_1, V_2, R_2, S_1

We can further distinguish whether the leptoquarks are scalar or vector. This could be accomplished in two ways. In the first one can study the angular distributions of the leptoquark decay products. In the second we can use the double asymmetry:

$$A_{LL} = \frac{(\sigma^{++} + \sigma^{--}) - (\sigma^{+-} + \sigma^{-+})}{(\sigma^{++} + \sigma^{--}) + (\sigma^{+-} + \sigma^{-+})}$$

where the first index refers to the electron helicity and the second to the quark helicity. Because scalars only have a non-zero cross section for σ^{++} and σ^{--} for scalar LQ's the parton level asymmetry for eq collisions is $\hat{a}_{LL} = +1$. Similarly, since vectors only have a non-zero cross section for σ^{+-} and σ^{-+} for vector LQ's $\hat{a}_{LL} = -1$.

To obtain observable asymmetries one must convolute the parton level cross sections with polarized distribution functions. Doing so will reduce the asymmetries from their parton level values of ± 1 so one must determine whether the observable asymmetries can distinguish between the leptoquark types. The expressions for the double longitudinal spin asymmetry A_{LL} are given in Ref. [11]. In Figures 4 and 5 we plot A_{LL} for the $e\gamma$ collider which started with $\sqrt{s}_{e^+e^-}$=1 TeV and with $\sqrt{s}_{e^+e^-}$=5 TeV respectively. To obtain these curves we used parameterizations of the *asymptotic* polarized photon distribution functions [26, 27], where it is assumed that Q^2 and x are large enough that the Vector Meson Dominance part of the photon structure is not important, but rather the behavior is dominated by the point-like $\gamma q\bar{q}$ coupling. In order to be consistent, we used a similar asymptotic parameterization for the unpolarized photon distribution functions as well [21], even though various sets of more correct photon distribution functions exist (*e.g.*, [22, 23, 24, 25]). We only used this asymptotic approximation in the unpolarized case for the calculation of the asymmetry, where it is hoped that in taking a ratio of the asymptotic polarized to the asymptotic unpolarized photon distribution functions, the error introduced will be minimized. Still, we suggest that our results be considered cautiously, at least in the relatively small LQ mass region. We note that in the asymptotic approximation, the unpolarized photon distribution functions have (not unexpectedly) a similar form to the polarized photon distribution functions.

In Fig. 4 and 5 we show asymmetries for 100% polarization and for 90% polarization which is considered to be achievable given the SLC experience. The error bars are based on an total integrated luminosity of 200 fb^{-1} for the 1 TeV case and 1000 fb^{-1} for the 5 TeV case. In these figures note that we are showing $-A_{LL}$ for the vector cases so that we can use a larger scale. Quite clearly, polarization would enable us to distinguish between vector and scalar. For the cases where there are two types of leptoquarks of the same chiral couplings, for example

the scalar isodoublet $\tilde{R}_2$ and scalar isotriplet S_3 or the vector isoscalar U_1 and vector isodoublet V_2, we could distinguish between them up to about 3/4 the kinematic limit.

Finally, one additional bit of information to further differentiate among the various possible leptoquarks is to search for the $\nu q'$ decay mode. This signature is quite similar to a supersymmetric particle decay (high p_T jet plus missing p_T) so that although it cannot be used to unambiguously determine the existence on leptoquarks, it can be used, in conjunction with the observation of an approximately equal number of eq events (as expected in some models) to provide further information on leptoquark couplings. Taken together, the leptoquark type can be uniquely determined. If more than one leptoquark were discovered, determining their properties would tell us their origin and therefore, the underlying theory.

V. SUMMARY

To summarize, we have presented results for single leptoquark production in $e\gamma$, e^+e^-, and $\mu^+\mu^-$ collisions. The discovery limits for leptoquarks is very close to the centre of mass energy of the colliding particles. It also appears that a polarized $e\gamma$ collider can be used to differentiate between the different models of LQs that can exist, essentially up to the kinematic limit. Furthermore, it is quite easy to distinguish scalar LQs from vector LQs for all LQ mass (given that the LQ is kinematically allowed). Thus e^+e^-, $e\gamma$, and $\mu^+\mu^-$ colliders have much to offer in the searches for leptoquarks. If leptoquarks were discovered, $e\gamma$ colliders could play a crucial role in unravelling their properties, and therefore the underlying physics.

VI. REFERENCES

[1] H1 Collaboration, I. Abt *et al.*, Nucl. Phys. **B396**, 3 (1993); H1 Collaboration, I. Ahmed *et al.*, Z. Phys. **C64**, 545 (1994).

[2] ZEUS Collaboration, M. Derrick *et al.*, Phys. Lett. **B306**, 173 (1993).

[3] D0 Collaboration, S. Abachi *et al.*, Phys. Rev. Lett. **72**, 965 (1994).

[4] CDF Collaboration, F. Abe *et al.*, Phys Rev. **D48**, 3939 (1993).

[5] ALEPH Collaboration, DeCamp *et al.*, Phys. Rept. **216**, 253 (1992).

[6] DELPHI Collaboration, P. Abreu *et al.*, Phys. Lett. **B316**, 620 (1993).

[7] L3 Collaboration, Adriani *et al.*, Phys. Rept. **236**, 1 (1993).

[8] OPAL Collaboration, G. Alexander *et al.*, Phys. Lett. **B263**, 123 (1991).

[9] See for example the ATLAS Technical Proposal, W.W. Armstrong *et al.*, CERN Report CERN/LHCC/94-43; J.L. Hewett, T.G. Rizzo, S. Pakvasa, H.E. Haber and A. Pomarol, *Proceedings of the Workshop on Physics at Current Accelerators and Supercolliders*, ed. J.L. Hewett, A.R. White, and D. Zeppenfeld, Argonne report ANL-HEP-CP-93-92, p. 539.

[10] M. A. Doncheski and S. Godfrey, Phys. Rev. **D49**, 6220 (1994); hep-ph/9608368.

[11] M. A. Doncheski and S. Godfrey, Phys. Rev. **D51**, 1040 (1995).

[12] O.J. Éboli, E.M. Gregores, M.B. Magro, P.G. Mercadante, and S.F. Novaes, Phys. Lett. **B311**, 147 (1993).

[13] H. Nadeau and D. London, Phys. Rev. **D47**, 3742 (1993); G. Bélanger, D. London and H. Nadeau, Phys. Rev. **D49**, 3140 (1994).

[14] J.L. Hewett and S. Pakvasa, Phys. Lett. **B227**, 178 (1989).

[15] F. Cuypers, hep-ph/9602355.

[16] For related papers see also: J. E. Cieza Montalvo and O.J.P. Éboli, Phys. Rev. **D47**, 837 (1993); T.M. Aliev and Kh.A. Mustafaev, Yad. Fiz. **58**, 771 (1991); V. Ilyin *et al.*, Phys. Lett. **B351**, 504 (1995); erratum **B352**, 500 (1995); Phys. Lett. **B356**, 531 (1995).

[17] W. Buchmüller, R. Rückl, and D. Wyler, Phys. Lett. **B191**, 442 (1987).

[18] M. Drees and R.M. Godbole, Proceedings of the Linear Collider Workshop, Waikoloa Hawaii, April 1993 (World Scientific); M. Drees, M. Krämer, J. Zunft, and P.M. Zerwas, Phys. Lett. **B306**, 371 (1993); O.J.P. Èboli, M.C. Gonzalez-Garcia, F. Halzen, and S.F. Novaes, Phys. Lett. **B301**, 115 (1993); A.C. Bawa and W.J. Stirling, Z. Phys. **C57**, 165 (1993); M. Glück, E. Reya, and A. Weber, Phys. Lett. **B298**, 176 (1993); P. Chen, T.L. Barklow and M.E. Peskin, SLAC report SLAC 5873 (1993; unpublished); K.J. Abraham, Phys. Lett. **B316**, 365 (1993); E. Laenen, S. Riemersma, J. Smith and W. L. van Neerven, preprint ITP-SB-93-46 and hep-ph/9308295 (1993, unpublished).

[19] I.F. Ginzburg *et al.*, Nucl. Instrum. Methods, **205**, 47 (1983); **219**, 5 (1984); C. Akerlof, Ann Arbor report UM HE 81-59 (1981; unpublished).

[20] Hadronic backgrounds in e^+e^- and $e\gamma$ collisions and associated references are given in M.A. Doncheski, S. Godfrey, and K.A. Peterson, Carleton Preprint OCIP/C-94-2 (hep-ph/9407348).

[21] A. Nicolaidis, Nucl. Phys. **B163**, 156 (1980).

[22] D.W. Duke and J.F. Owens, Phys. Rev. **D26**, 1600 (1982).

[23] M. Drees and K. Grassie, Z. Phys. **C28**, 451 (1985); M. Drees and R. Godbole, Nucl. Phys. **B339**, 355 (1990).

[24] M. Glück, E. Reya and A. Vogt, Phys. Lett. **B222**, 149 (1989); Phys. Rev. **D45**, 3986 (1992); Phys. Rev. **D46**, 1973 (1992).

[25] H. Abramowicz, K. Charchula, and A. Levy, Phys. Lett. **B269**, 458 (1991).

[26] J.A. Hassan and D.J. Pilling, Nucl. Phys. **B187**, 563 (1981).

[27] Z. Xu, Phys. Rev. **D30**, 1440 (1984).

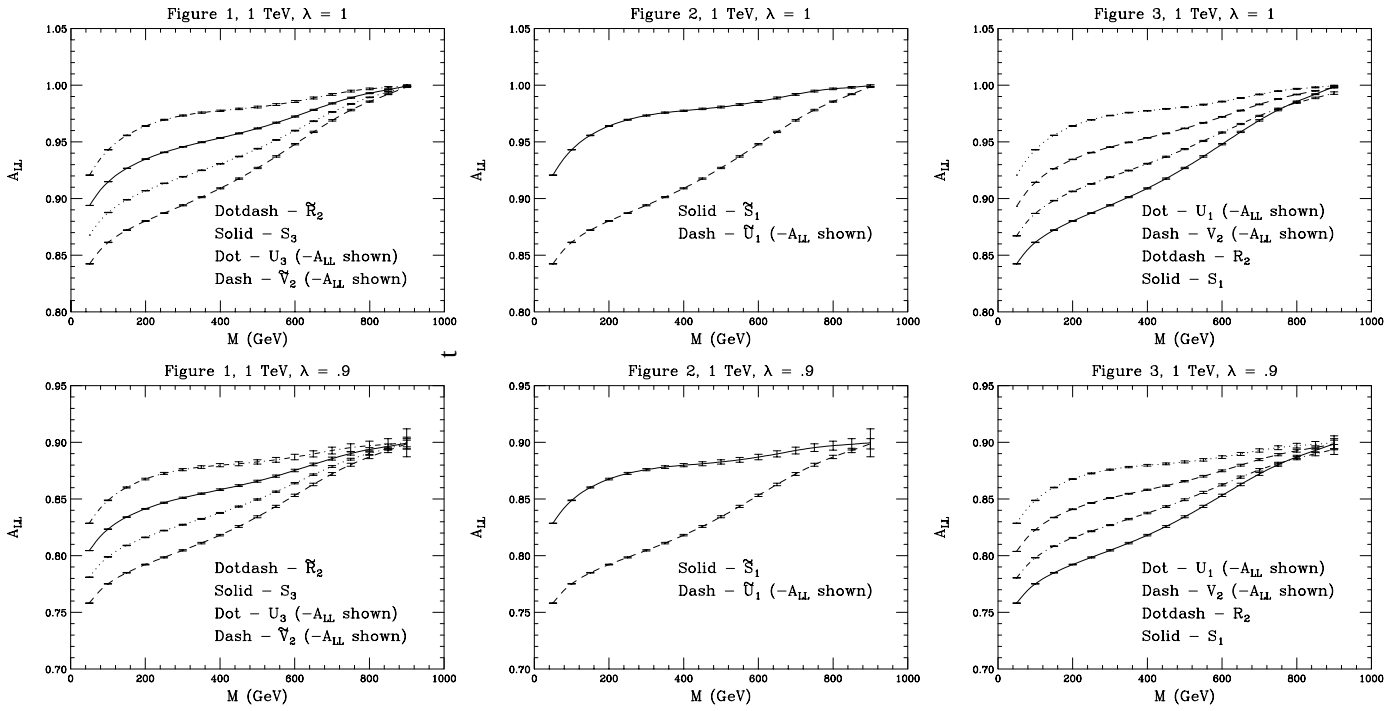

Figure 4: A_{LL} vs M_{LQ} for a 1 TeV $e\gamma$ collider. The statistical errors are based on 200 fb^{-1}. The top row is for 100% polarization and the bottom row for 90% polarization. The first column is for LQ's which couple only to left-handed electrons, the second column is for LQ's which couple only to right-handed electrons, and the third column is for LQ's which couple to both left and right-handed electrons.

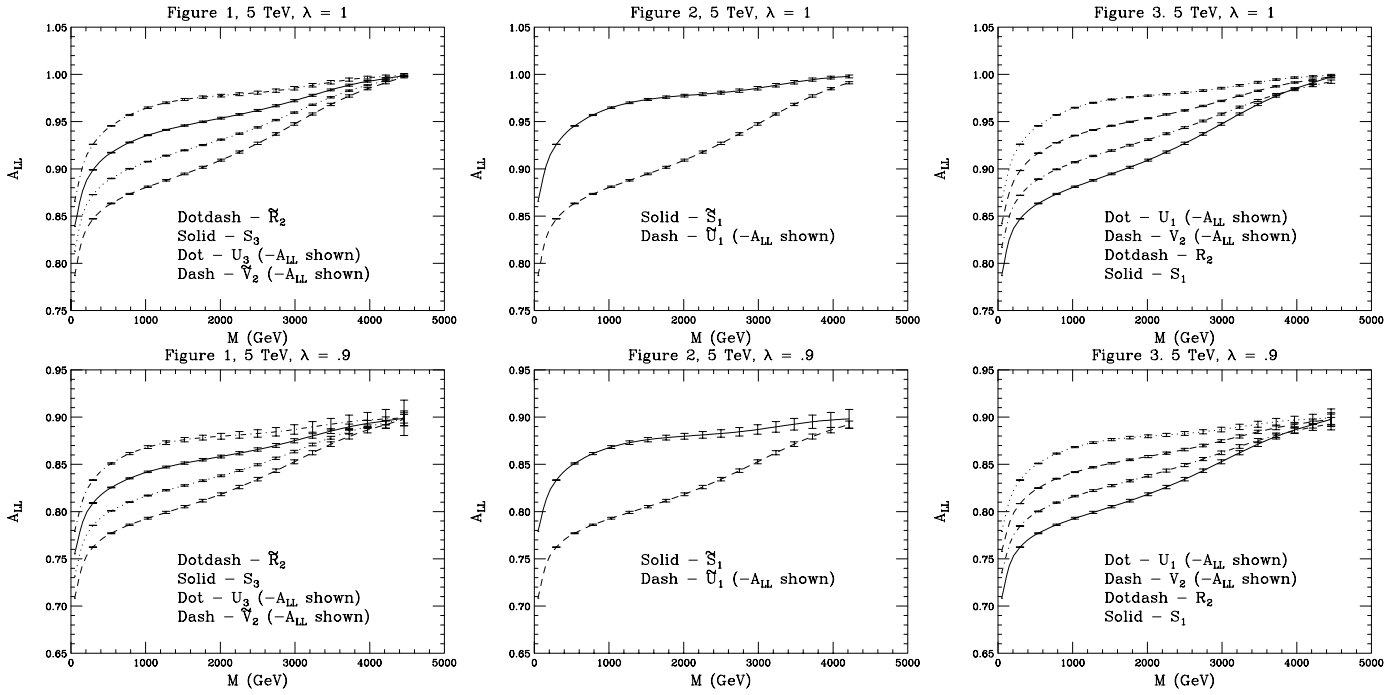

Figure 5: A_{LL} vs M_{LQ} for a 5 TeV $e\gamma$ collider. The statistical errors are based on 1000 fb^{-1}. The top row is for 100% polarization and the bottom row for 90% polarization. The first column is for LQ's which couple only to left-handed electrons, the second column is for LQ's which couple only to right-handed electrons, and the third column is for LQ's which couple to both left and right-handed electrons.